

# Phase Separation of Poly(*N*-isopropylacrylamide) Solutions and Gels Using a Near Infrared Fiber Laser

Michael E. DeRosa,<sup>1</sup> Rebecca L. DeRosa,<sup>2</sup> Lisa M. Noni,<sup>1</sup> Erin S. Hendrick<sup>3</sup>

<sup>1</sup>Corning Incorporated, Science and Technology Division, Corning, New York

<sup>2</sup>Inamori School of Engineering, Materials Science and Engineering, Alfred University, Alfred, New York

<sup>3</sup>Department of Textiles and Apparel, Cornell University, Ithaca, New York

Received 3 October 2006; accepted 11 January 2007

DOI 10.1002/app.26251

Published online 3 May 2007 in Wiley InterScience (www.interscience.wiley.com).

**ABSTRACT:** We used a tunable near infrared fiber laser in the wavelength range of 1533–1573 nm to induce photo-thermal phase changes in poly(*N*-isopropylacrylamide) (PNIPAM) aqueous solutions and hydrogels. The laser induces the hydrophilic to hydrophobic transition of the polymer by heating the surrounding water. We report our observations of the phase changes based on using a novel fiber backreflectance method coupled with visual cloud point measurements. At 1533 nm the phase transition was induced at the end of a single mode optical fiber with

9 mW of power at an ambient temperature of 24°C. We found that the power required to reach the lower critical solution temperature was inversely proportional to the absorption spectrum of water. In addition, phase changes in both solutions and gels occurred very rapidly (<1 s) as the laser was turned on and off. © 2007 Wiley Periodicals, Inc. *J Appl Polym Sci* 105: 2083–2090, 2007

**Key words:** hydrogels; phase separation; polyNIPAM; photothermal; near infrared; fiber laser; UV-vis spectroscopy

## INTRODUCTION

Poly(*N*-isopropylacrylamide) (PNIPAM) is a thermoreversible polymer that undergoes a change in its physical properties at a lower critical solution temperature (LCST), which is near 32°C.<sup>1</sup> At the LCST, aqueous PNIPAM solutions undergo a hydrophilic to hydrophobic coil-globule transformation; while cross-linked PNIPAM hydrogels go from a swollen expanded state to a collapsed, contracted structure. The change is reversible and repeatable making PNIPAM useful for applications such as coatings for thermally responsive surfaces for protein,<sup>2</sup> enzyme,<sup>3</sup> and cell attachment,<sup>4</sup> drug delivery<sup>5,6</sup> and control of flow in microfluidic systems.<sup>7</sup>

When the temperature is below the LCST, the polymer exists in an expanded hydrophilic state. However, as the temperature is raised above the LCST, the polymer goes through an abrupt conformational rearrangement resulting in a collapsed hydrophobic state. The conformational change is a result of the break-up of the network of hydrogen-bonded water surrounding the hydrophobic segments of the polymer chain. Below the LCST, the hydrogen-bonded network of water serves to stabilize and extend the chain. As the water network is disrupted by thermal energy, van

der Waals attractive forces between hydrophobic domains contribute to chain collapse.<sup>8</sup>

PNIPAM hydrogels also undergo a phase transition near 32°C. The gel is an expanded hydrophilic polymer network in water. Above this critical temperature at 32°C, the gel shrinks rapidly as the network becomes hydrophobic.

A majority of the studies on the phase behavior of PNIPAM polymer solutions and gels have been done by bulk heating of the entire solution or gel. However, several groups have reported that it is possible to induce localized phase separation by photothermal heating of the material in a localized region by using a laser. Many of the studies relied on an absorbing additive to heat the localized area around the PNIPAM molecules. The earliest reference to photothermal heating of PNIPAM was reported by Suzuki and Tanaka.<sup>9</sup> They created PNIPAM hydrogels with the chromophore trisodium salt of copper chlorophyllin, which they covalently attached to the gel network. The chromophore absorbs in the visible portion of the spectrum and is directly heated with an argon-ion laser operating at 488 nm. The heat generated by the absorption of the laser power induces localized volume changes in the gel. More recently, Nayak and Lyon<sup>10</sup> used a HeNe laser to induce a phase transition in dye-labeled PNIPAM microgels. In this case, they covalently bound malachite green to PNIPAM microgels. Malachite green has a strong absorption peak at 620 nm; a HeNe laser at 632 nm was used to induce the photothermal phase transition in the gel. In another study, Sershen et al.<sup>11</sup> added gold nano-

Correspondence to: M. E. DeRosa (derosame@corning.com).

particles or silica-gold core-shell nanoparticles to a PNIPAM gel to absorb radiation at 532 nm and 832 nm, respectively, to heat the gel. They concluded that by incorporating dopants with independent optical resonances they could selectively induce optically driven phase changes in the copolymer. Finally, Gorelikov et al.<sup>12</sup> did a similar experiment where they combined PNIPAM with gold nanorods that were designed to absorb light in the near-IR (NIR) range. They stabilized the composite between polymer and the gold nanorods using attractive electrostatic forces between the positively charged gold nanorods and negatively charged PNIPAM. To induce the phase change, the group heated the solution to 30°C and then applied laser radiation at 810 nm and 30 W. They were able to detect the percent volume shrinkage due to the photothermal heating as well as obtain repeatable measurements upon cycling the laser on and off.

Other researchers have shown that it is possible to induce photothermal phase separation of PNIPAM solutions and gels by directly heating the water with a laser instead of adding absorbing additives to the polymer. Ishikawa et al.<sup>13</sup> demonstrated photothermal heating of aqueous PNIPAM solutions by heating the water using a Nd : YAG laser at 1064 nm. They used the localized heating from the laser to create PNIPAM microparticles. The microparticle formation was found to be fast and reversible. They were also able to control the size of the microparticle from 2 to 9  $\mu\text{m}$  by controlling the polymer concentration, laser power, and solution temperature. Using the same methods, Hofkens et al.<sup>14</sup> demonstrated the assembly of PNIPAM microparticles upon prolonged application of highly focused laser radiation at 1064 nm to aqueous solutions of PNIPAM. Other groups have also used 1064 nm to photothermally heat PNIPAM gels to undergo phase transitions.<sup>15,16</sup>

Though photothermal phase separation studies have been conducted using lasers operating at 1064 nm, water has a much higher absorption in the near infrared between 1350 and 1600 nm. Therefore, phase separation should occur at a much lower intensity using a NIR laser than is required by using a Nd:YAG source. In this study we demonstrate the use of a tunable NIR fiber laser to induce a localized phase change in PNIPAM solutions and gels using wavelengths in the range of 1533–1573 nm. We report our observations of phase separation using a novel fiber optic back reflectance technique coupled with visual cloud point methods.

## EXPERIMENTAL SECTION

### Sample preparation

Poly(*N*-isopropylacrylamide) ( $M_n = 20,000\text{--}25,000$  g/mol), *N*-isopropylacrylamide (NIPAM), methylenebisacrylamide (BIS), ammonium persulfate (APS),

and *N,N,N',N'*-tetramethylethylenediamine (TEMED) were used as received from Sigma-Aldrich (St. Louis, MO) to make solutions and gels. Solutions of poly(*N*-isopropylacrylamide) (PNIPAM) were made by dissolving the polymer in distilled water at concentrations of 1, 3, 6, 8, and 10 wt %. Gels were made by dissolving 1.13 g of monomer (NIPAM), 0.006 g of crosslinker (BIS), and 0.05 g of initiator (APS) in distilled water while stirring in a beaker at 25°C. TEMED (0.01 g) was added to the solution while being stirred. Gels formed in  $\sim 2.5$  min. The level of crosslinker was adjusted to produce gels with a range of crosslink density. In this study we made gels with a molar ratio of BIS/NIPAM from 0.002 to 0.02.

### NIR spectroscopy

The near infrared spectra of a 6 wt % PNIPAM solution and water only were taken to determine the absorption characteristics in the wavelength region where the laser will be used. A cuvette with a 1 mm pathlength was filled with the liquid and loaded into the spectrometer (Perkin-Elmer Lambda 900, Waltham, MA). An air background was taken to subtract out the effect of reflections from the front and rear surfaces of the cuvette. The sample was scanned and the absorbance spectrum was collected from 400 to 2500 nm.

### DSC measurements

A Seiko DSC 220 differential scanning calorimeter (Torrance, CA) was used to examine the phase transition of a 6 wt % PNIPAM aqueous solution. A 10  $\mu\text{L}$  sample was cycled twice between 15°C and 50°C at a rate of 3°C/min. On heating, the sample showed a clear endothermic peak at 33°C while on cooling the sample showed an exothermic peak at 31°C.

### Cloud point measurements

The lower critical solution temperature of solutions and gels was determined by using a visual cloud point method. A cuvette with a 1 mm path length was filled with PNIPAM solution and placed on a microscope hot stage (Mettler Toledo model FP82HT, Columbus, OH). The temperature was increased manually with the temperature controller and allowed to equilibrate. The sample was observed through the window of the hot stage and the LCST was recorded as the temperature at which the sample began to show the initial signs of becoming translucent.

Gels of varying amounts of crosslinker were placed between glass slides using a 1.5 mm O-ring spacer and placed on the hot stage. The LCST of the gels was determined by using the same method as the solutions.

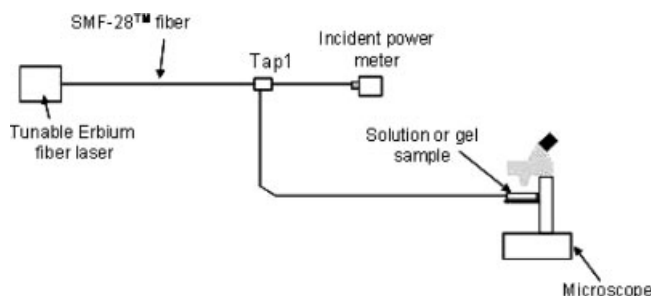


**Figure 1** Fiber laser test setup for photothermal phase separation experiments of PNIPAM solutions and hydrogels.

### Fiber laser measurements

The laser test setup used in our study is shown in Figure 1. A fiber laser (IPG Photonics, Oxford, MA, model ELT-4 AM) was used for all phase separation and backreflectance measurements. The wavelength output of the laser is tunable from 1533.00 nm to 1573.00 nm. We used SMF-28™ fiber (Corning Inc., Corning, NY) with a mode field diameter (MFD) of 10.5  $\mu\text{m}$  at 1550 nm. The MFD changes with wavelength across the tunable range of the laser. Therefore, at different wavelengths we report the intensity rather than the power at the phase separation point to make a direct comparison of where the phase transition occurs. At 1533, 1550, and 1573 nm the MFD is 10.4, 10.5, and 10.6 microns, respectively.

The laser was spliced to a 1/99 tap coupler. The tap leg was connected to a power meter which, after calibration, monitored the input power to the sample. The main output leg of the coupler was sent to the PNIPAM solution or gel. The sample was placed under a microscope (Nikon Optiphot-2, Nikon Instruments, Melville, NY) and the end of the fiber was monitored via video camera as the laser power was increased. The lowest power level at which localized phase separation was observed was taken to be the point of the photothermal LCST. We performed this experiment for all solution concentrations and gel crosslink densities at an ambient temperature of 24°C.

### Fiber backreflectance measurements

The setup for fiber backreflectance measurements is shown in Figure 2. The laser was spliced to one leg of a 50/50 coupler. The output fiber has a flat cleave on it and is embedded into the solution or gel sample. An InGaAs detector was attached to the second leg of the 50/50 coupler to monitor the reflected power sent back through the fiber endface which was embedded in the sample. We increased the power and recorded the reflected power intensity at each power level for 30 s. The reflected signal and standard deviation of the reflected signal was then recorded. We then plot-

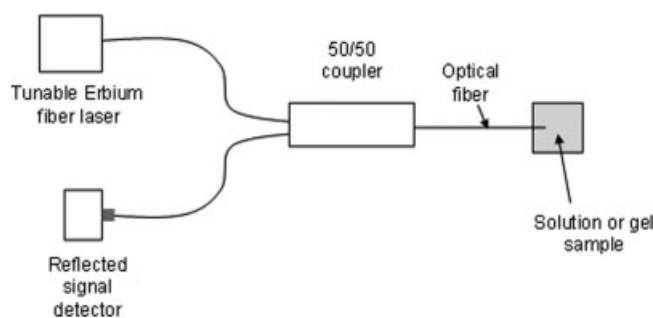


**Figure 2** Photothermal backreflectance setup for determining phase separation at 1550 nm.

ted the standard deviation of the signal as a function of laser power. At the phase separation point, the signal becomes noisy due to scattering in the sample. The jump in the standard deviation of the reflected signal was taken to be the phase separation point. All backreflectance tests were performed at 1550 nm.

## RESULTS AND DISCUSSION

### Cloud point measurement

The results of the cloud point measurements using the hot stage are shown in Figures 3 and 4 for the solutions and gels, respectively. We found the LCST of the PNIPAM solution to be near 33°C and essentially independent of polymer concentration. An LCST of 33°C compares to 32°C reported in the literature.<sup>1</sup> The flat LCST behavior has been observed by others<sup>17,18</sup> and the values of the LCST via cloud point are consistent with our DSC results.

The phase behavior of the PNIPAM gels, shown in Figure 4, is independent of the level of crosslinker.

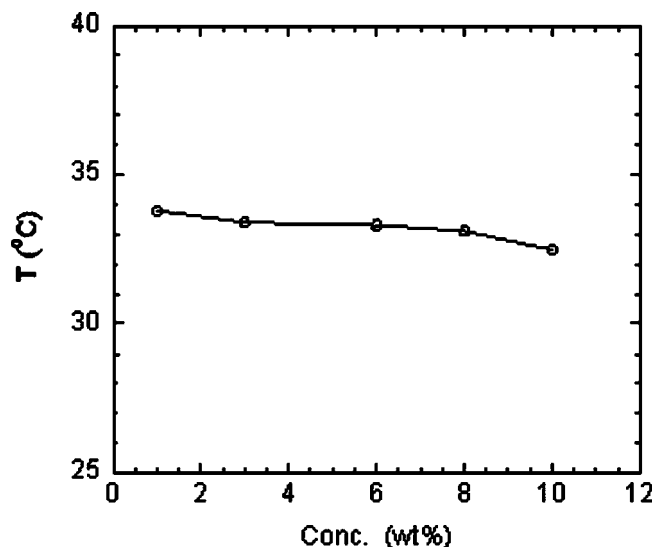


**Figure 3** Lower critical solution temperature (LCST).

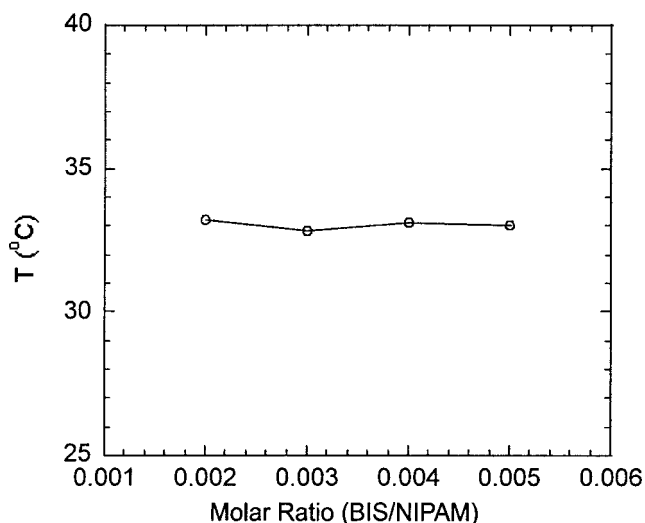


**Figure 4** Cloud point phase diagram of PNIPAM gels as a function of the amount of crosslinker.

The LCST is near 33°C which is the same value found for the solutions.

#### Photothermal phase separation-PNIPAM solutions

The NIR spectrum of a 6% solution of PNIPAM and water is shown in Figure 5. The absorption due to the O—H vibration overtone mode of the water in the region of 1380–1650 nm is so dominant that the contribution of the PNIPAM can not be detected. Therefore, any photothermal action that took place in our experiments in the region of 1533–1573 nm was almost entirely due to heating of the water. Previous studies that used 1064 nm to induce photothermal heating of the PNIPAM gels and solutions would require 108 times the laser intensity as that at 1533 nm to heat the material to the LCST. The advantage of using less power at these longer wavelengths means that we reduce the chances of damaging the material should the laser come in contact with any highly absorbing impurities. We also may be able to integrate low power lasers with other technologies such as microfluidic systems<sup>2,7</sup> since fairly inexpensive single wavelength, fiber pigtailed laser diodes from 1533 to 1573 nm are commercially available. Other inexpensive fiber laser sources from 1450 to 1480 nm are also available and by using these wavelengths we could further reduce the power requirement to induce the photothermal phase needed at 1533 nm by another factor of two.

The photothermal phase separation of a 6 wt % PNIPAM solution is shown in Figure 6. We began to see phase separation at 9 mW of power [Fig. 6(b)] at an ambient temperature of 24°C. This power level is taken to be the photothermal LCST. At 500× magnification we could just barely detect small droplets of

phase separated polymer. The rate at which phase separation occurred was not measured but appeared to be very rapid (i.e., <1 s).

What is not apparent in the figures is that we observed the droplets to be moving away from the end of the fiber. As the power was increased to 14.5 mW and then 20 mW, we clearly established a circular convection current in the solution. As phase separated polymer drifted out of the heated zone it disappeared as the temperature fell back below the LCST. As new solution entered the heated zone, new droplets would rapidly form.

We were not able to characterize the temperature gradient in the sample but using the LCST as measured from cloud point and DSC we can calculate a local peak temperature at the endface of the fiber as a function of power. Given the LCST to be 33°C and the ambient temperature to be 24°C, we induced a temperature rise of 9°C with 9 mW at the mode field diameter of SMF-28<sup>®</sup>. This translates into a photothermal heating coefficient of 1°C/mW.

As we increased the power of the laser above the LCST, we most likely increased the temperature of the center portion of the phase separated region. However, due to scattering it is difficult to measure the absolute temperature in this area. As the power is increased we move the spatial boundary of the LCST outward as can be seen in Figure 6(c,d). The outer edge of the oblong shaped region marks the LCST and demarcates the boundary between where PNIPAM is in its hydrophilic or hydrophobic configuration. The characteristic shape of the region we observed could be due to thermal lensing caused by photothermal localized heating.

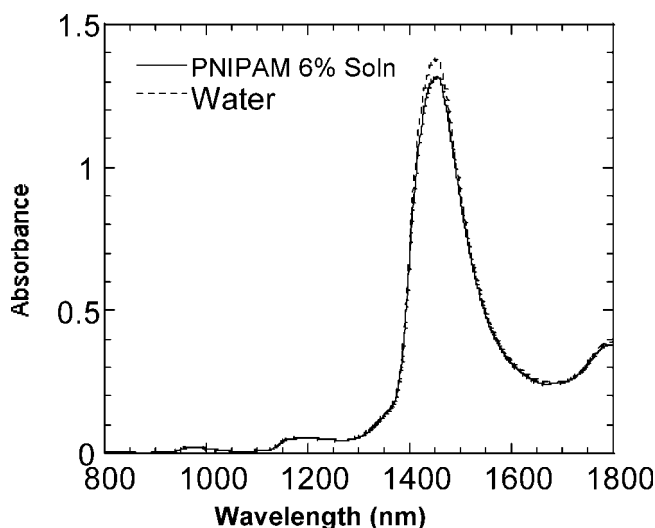


**Figure 5** Near IR spectra of a 6 wt % solution of PNIPAM in distilled water compared with that of water alone. The path length is 1 mm.

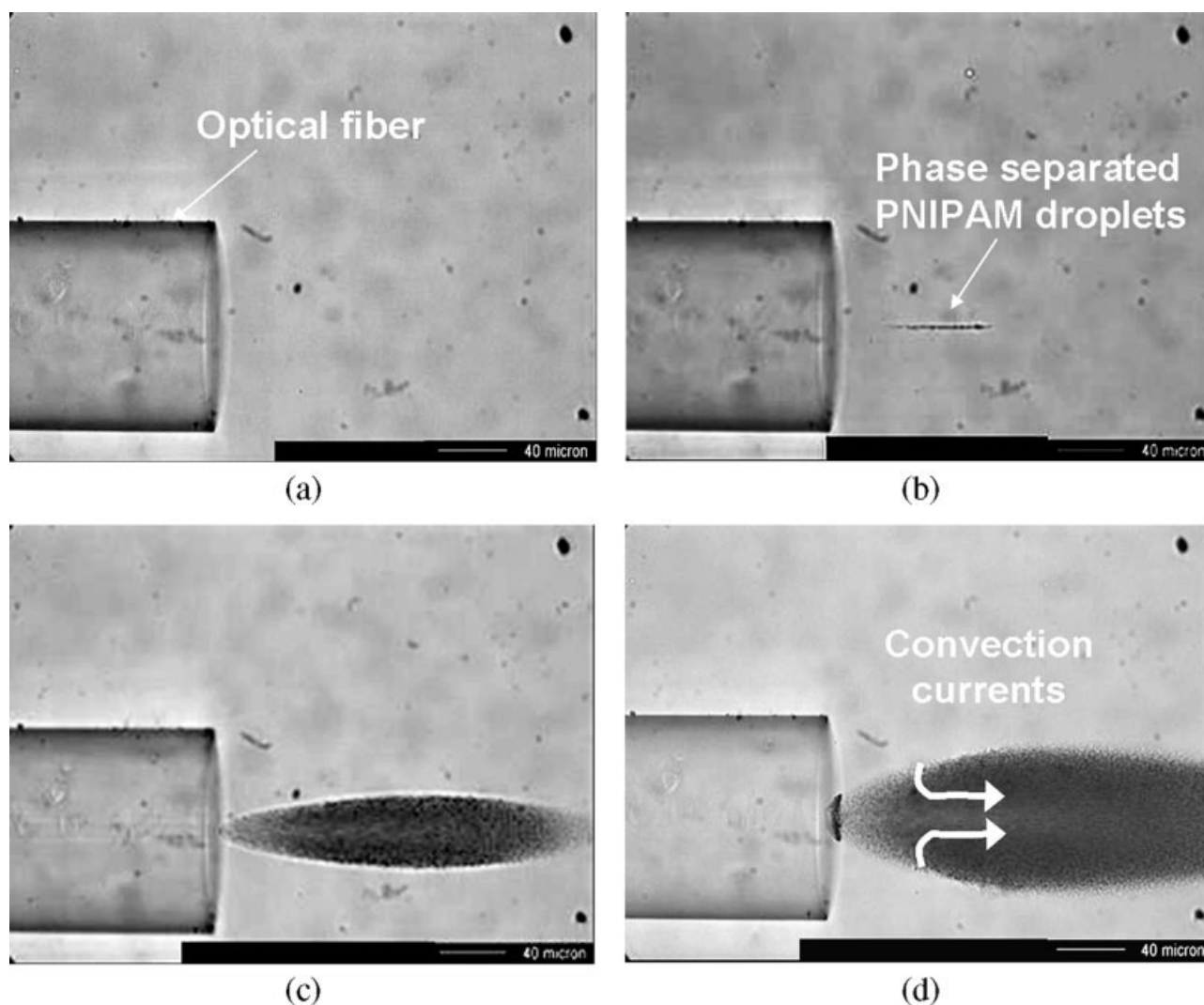


**Figure 6** Photothermal phase separation of 6 wt % PNIPAM solution at 1533 nm at (a) 0 mW, (b) 9 mW, (c) 14.5 mW, and (d) 20 mW. Images were taken at 500 $\times$  magnification.

A photothermal phase diagram for PNIPAM solutions is shown in Figure 7. The phase diagram is relatively flat above a concentration of 3 wt %. At 1 wt % the power required to reach the LCST was higher. We believe that this is due to the fact that we used a visual method with the microscope and camera to determine the initial phase separation behavior. The size of the phase separated region is only on the order of several microns and at 1 wt % concentration the change at the LCST is very faint. Therefore, we believe that we had to overshoot the power needed to visually observe the phase change for the 1% solution.

Alternatively, we demonstrated that we could detect the phase change with the fiber backreflectance method. A plot of the standard deviation of the reflected laser signal is shown in Figure 8 for three solution concentrations. The results show that the increase in standard deviation of the average signal, i.e., the variability of the signal, increases in a step-

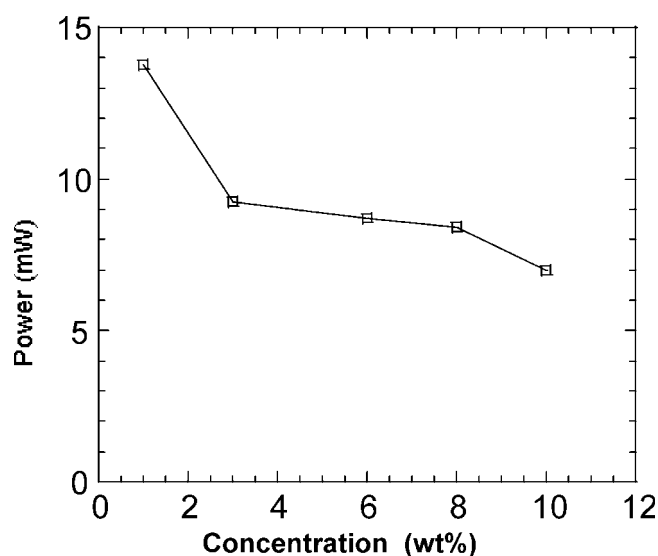


**Figure 7** Photothermal phase diagram of PNIPAM solutions at 1533 nm.

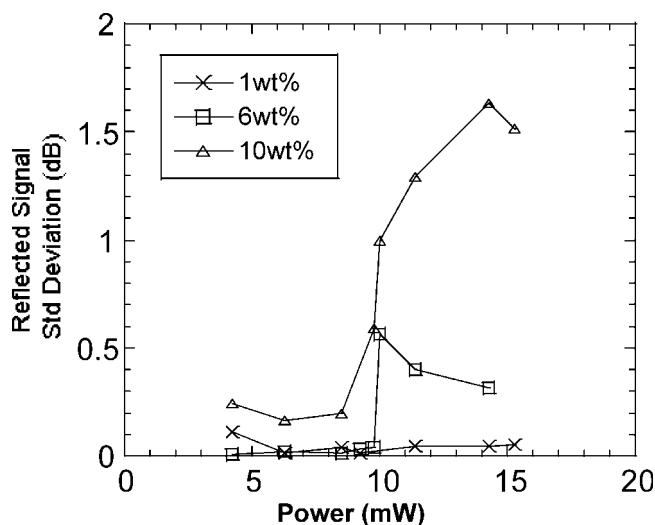


**Figure 8** Fiber backreflectance measurement of PNIPAM solutions showing the standard deviation of the reflected signal versus laser power. The phase transition occurs at the step-jump in the data.

like function at the phase transition point between 9 and 10 mW. This value is in agreement with what we observed using the microscope to detect photothermal phase separation. Also, the photothermal phase transition occurs at the same incident power of  $\sim 9.5$  mW for all concentrations. Finally, the magnitude of the standard deviation at the transition increases with increasing concentration. However, at some point this will level off as scattering is maximized. At 1 wt %, even the fiber technique could barely detect the phase transition point which is what we experienced using the visual method.

The photothermal phase transition is also sensitive to the wavelength used to induce phase separation.

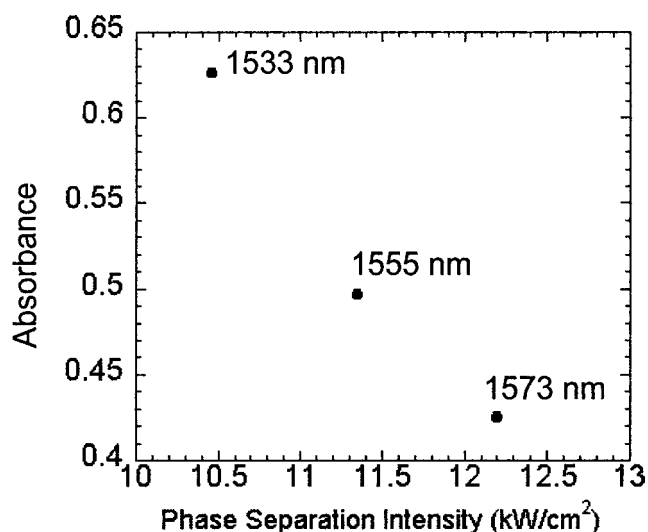


**Figure 9** Absorbance of water at 1533, 1555, and 1573 nm versus laser intensity at the LCST of a 6 wt % PNIPAM solution.

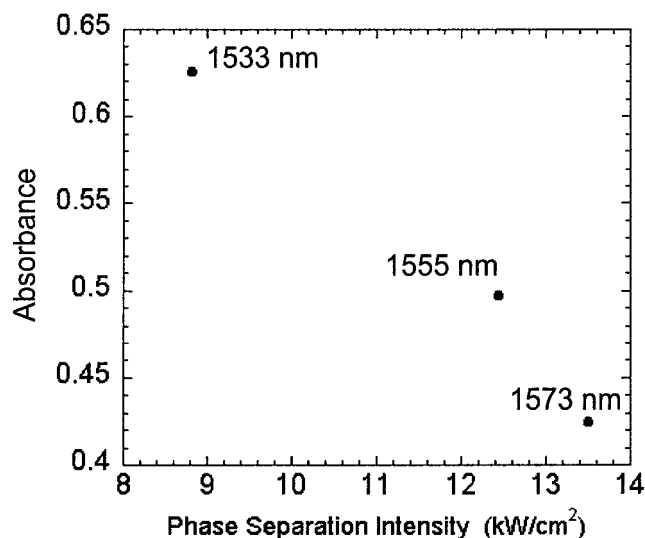


**Figure 10** Absorbance of water at 1533, 1555, and 1573 nm versus laser intensity at the LCST of a 0.005 BIS/NIPAM gel.

We used heating wavelengths of 1533, 1555, and 1573 nm in our experiments. In this portion of the spectrum, we are exciting the long wavelength tail of the O—H overtone as we discussed earlier. Figure 9 shows that the laser intensity required to reach the photothermal LCST of the solution increases as the absorbance of water decreases going from 1533 to 1573 nm. We observed the same trend for the PNIPAM hydrogels which is shown in Figure 10.

#### Photothermal phase separation-PNIPAM gels

We observed that the power required to induce the phase transition was independent of crosslinker con-

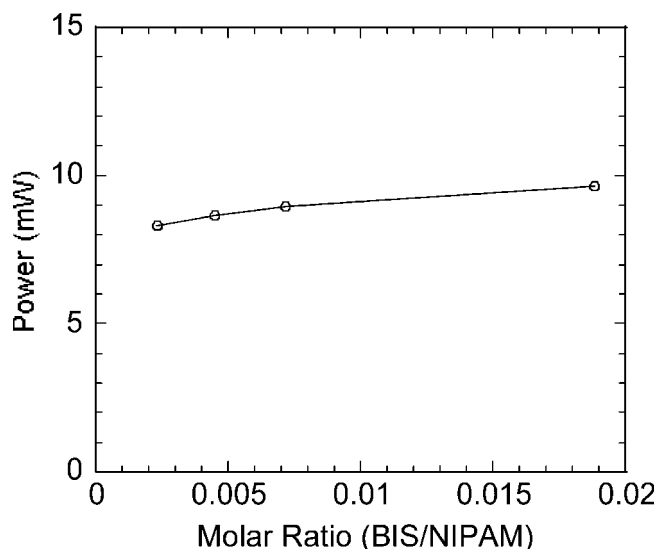


**Figure 11** Photothermal phase diagram of PNIPAM gels showing the power required to reach the transition point as a function of crosslinker content.

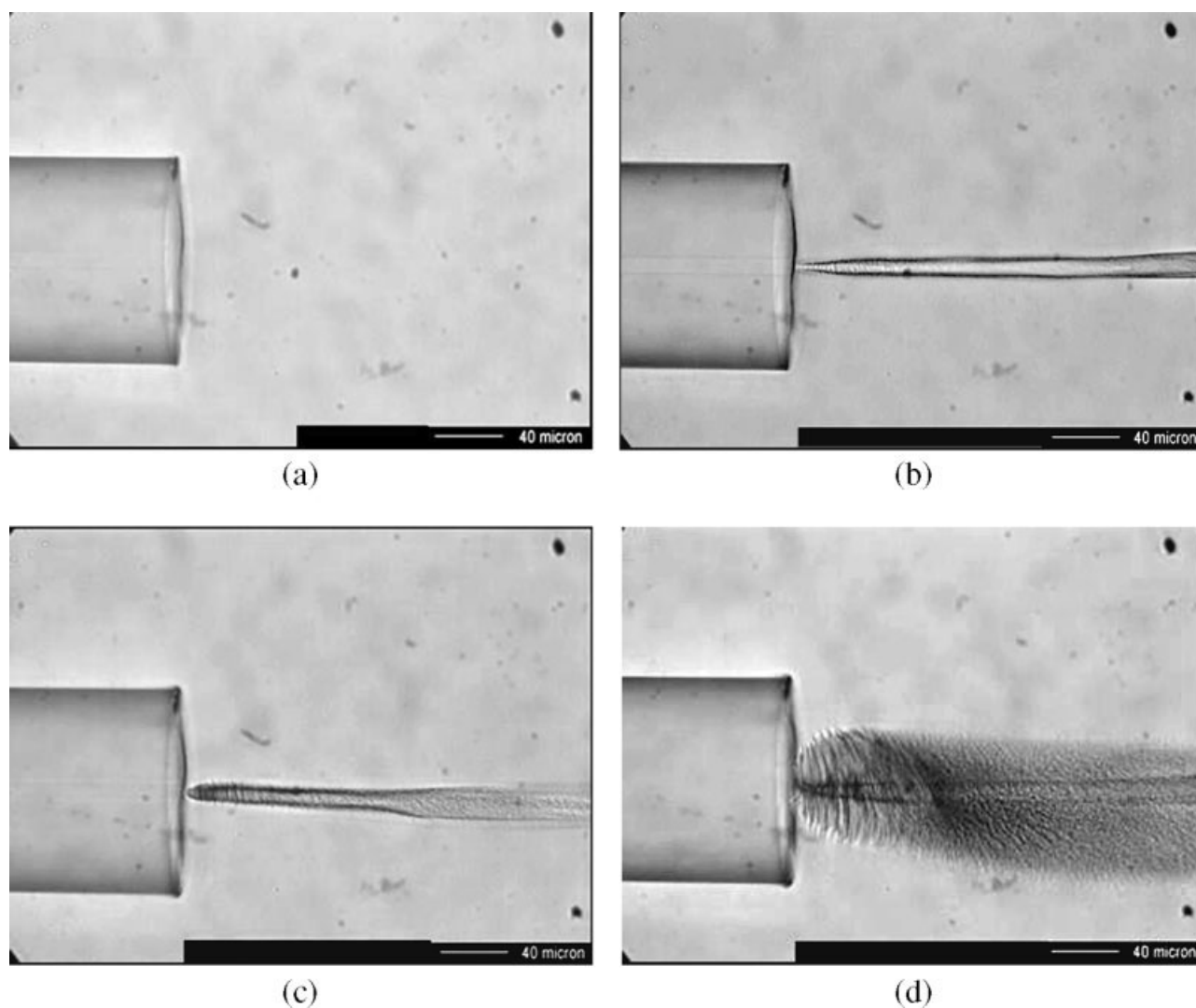


**Figure 12** Photothermal phase change behavior at 1533 nm of PNIPAM gel with 0.0039 BIS/NIPAM crosslinker/monomer ratio. Optical powers at the end of the fiber are (a) 0 mW, (b) 12 mW, (c) 13 mW, and (d) 21.5 mW.

tent. This is shown in Figure 11. The power required to reach the transition is nearly the same for the gels as it is for the solutions. This is also consistent with our cloud point observations.

Though the gels exhibited a transition point at nearly the same optical power as the solutions, they showed a dramatically different morphology at the photothermal transition point. Figure 12 shows the gel at the end of the optical fiber as a function of input power.

As phase separation occurred, there did not appear to be any droplets forming as was clearly seen in the solutions. Also, the shape of the phase separated domain was shaped more like a tube growing off the end of the fiber instead of an oval shaped region like we observed in the solutions. Finally, at higher powers we did not observe any convection currents. The phase separated region was essentially motion-

less due to restricted molecular motion through cross-linking. When the laser was turned off, the structure disappeared rapidly in  $<1$  s.

The difference in phase change morphology at the end of the fiber for the solutions and gels could be due to the structures that form reversibly for each at the LCST. PNIPAM polymer undergoes a coil to globule transition at the LCST. The transition from hydrophilic to hydrophobic behavior of the polymer causes it to collapse out of solution and form droplets with other phase separated polymer molecules. As the laser intensity is increased, there appears to be a certain amount of thermal blooming or scattering that occurs. Hence, we observe an oblong oval shape localized phase region which is a manifestation of the defocused beam profile. Such photothermal blooming effects have been reported in transparent organic optical materials at these wavelengths.<sup>19</sup>

## CONCLUSION

We demonstrated that we could induce localized photothermal phase separation in PNIPAM solutions and gels using a near infrared fiber laser at wavelengths from 1533 to 1573 nm. We detected this transition visually and by using a new fiber backreflection technique. We observed that the phase separated solutions exhibited discrete droplets that flowed away from the fiber tip due to convection currents while the phase separated gel was a stationary globule structure that was fixed to the tip of the fiber. The transitions we observed were caused by localized photothermal heating due to excitation of the O—H overtone water band which has a maximum absorption near 1450 nm. By using this portion of the spectrum, the overall intensity required to induce the phase transition is much lower than that reported in previous studies using 1064 nm. It therefore may be possible to integrate low cost NIR fiber lasers into devices containing switchable thermoreversible aqueous materials used for applications such as drug delivery, protein attachment to surfaces, and microfluidics.

The authors thank Marie Bryhan, Michael Sorensen, and Stephan Logunov for their assistance and helpful discussions during this project.

## References

1. Schild, H. G. *Prog Polym Sci* 1992, 17, 163.
2. Huber, D. L.; Manginell, R. P.; Samara, M. A.; Il-Kim, B.; Bunker, B. C. *Science* 2003, 301, 352.
3. Dong, L. C.; Hoffman, A. S. *J Controlled Release* 1986, 4, 223.
4. Yamato, M.; Konno, C.; Utsumi, M.; Kikuchi, A.; Okano, T. *Biomaterials* 2002, 23, 561.
5. Hoffman, A. S.; Afrassiabi, A.; Dong L. C. *J Controlled Release* 1986, 4, 213.
6. De las Heras Alarcon, C.; Pennadam, S.; Alexander, C. *Chem Soc Rev* 2005, 34, 276.
7. Saitoh, T.; Suzuki, Y.; Hiraide, M. *Anal Sci* 2002, 18, 203.
8. Lin, S.-Y.; Chen, K.-S.; Run-Chu, L. *Polymer* 1999, 40, 2619.
9. Suzuki, A.; Tanaka, T. *Lett Nature* 1991, 346, 345.
10. Nayak, S.; Lyon, L. A. *Chem Mater* 2004, 26, 2623.
11. Sershen, S. R.; Westcott, S. L.; Halas, N. J.; West, J. L. *Appl Phys Lett* 2002, 80, 4609.
12. Gorelikov, I.; Field, L. M.; Kumacheva, E. *J Am Chem Soc* 2004, 126, 15938.
13. Ishikawa, M.; Misawa, H.; Kitamura, N.; Fujisawa, R.; Masuhara, H. *Bull Chem Soc Jpn* 1996, 69, 59.
14. Hofkens, J.; Hotta, J.; Sasaki, K.; Masuhara, H.; Iwai K. *Langmuir* 1997, 13, 414.
15. Goto, T.; Kato, J.; Yamashita, T. *J Photopolym Sci Technol* 2004, 17, 285.
16. Yan, H.; Fujiwara, H.; Sasaki, K.; Tsujii, K. *Angew Chem Int Ed Engl* 1951, 2005, 44.
17. Milewska, A.; Szydowski, J.; Rebelo, L. P. N. *J Polym Sci* 2003, 41, 1219.
18. Okada, Y.; Tanaka, F. *Macromolecules* 2005, 38, 4465.
19. DeRosa, M. E.; Logunov, S. L. *Appl Opt* 2003, 42, 2683.